Referee #2

We thank the reviewer for a thoughtful and thorough review of our manuscript (ESSD-2023-87: SinoLC-1: the first 1-meter resolution national-scale land-cover map of China created with the deep learning framework and open-access data). The suggestions and comments are listed in **bold** type. The modified words or materials are marked as blue color in the revised manuscript. The item-by-item responses to all comments are listed below.

General comments:

The authors of this manuscript took such a tremendous effort to classify land cover of China in a very high (1m) resolution. However, the uncertainty of training datasets, the reproducibility of methods and the independence of validation were not clear.

Response:

We appreciate your considerable comments and suggestions which help to clarify the scientific significance of SinoLC-1 land-cover dataset and expand its applicability. We have carefully considered all of the comments and suggestions listed below and tried our best to improve the manuscript focusing on clarifying the certainty of the training set, the reproducibility of the method, and the independence of validation.

Suggestions and comments:

(1) This manuscript utilized 3 global-scale land cover products as training samples, but the mapping accuracy of them in China is uncertain especially considering that a small number of observations in China were included to generate these maps. Also, the uncertainty of the SinoLC-1 in the Southwest, Northwest and North regions due to unmatched training data and outdated VHR images need to be considered.

Response:

We appreciate the reviewer for providing relevant and constructive comments and suggestions. To be clearer and in accordance with your concerns, we made major revisions and added materials as follows:

Firstly, to analyze the uncertainty of three global land-cover products, which were used to generate the SinoLC-1, more rigorously, we added two widely used open-access validation datasets to assess the accuracy of five global-scale products (including three utilized 10-m products and other two 30-m products) across China. According to your concerns in **Comments 2 and 9**, we have fully evaluated their user accuracy, overall accuracy, and kappa coefficient for each land-cover type in China, which are presented in Table R2-5, Figure R2-17, and Figure R2-18. We also analyzed their potential impact on the production process of SinoLC-1 comprehensively. Figure R2-1 shows the supplemented workflow added to comprehensively evaluate the accuracy and uncertainty of the SinoLC-1 and other land-cover products. The detailed material and descriptions are demonstrated in response to **Comments 2 and 9** (pages 2 and 19 of this response letter).

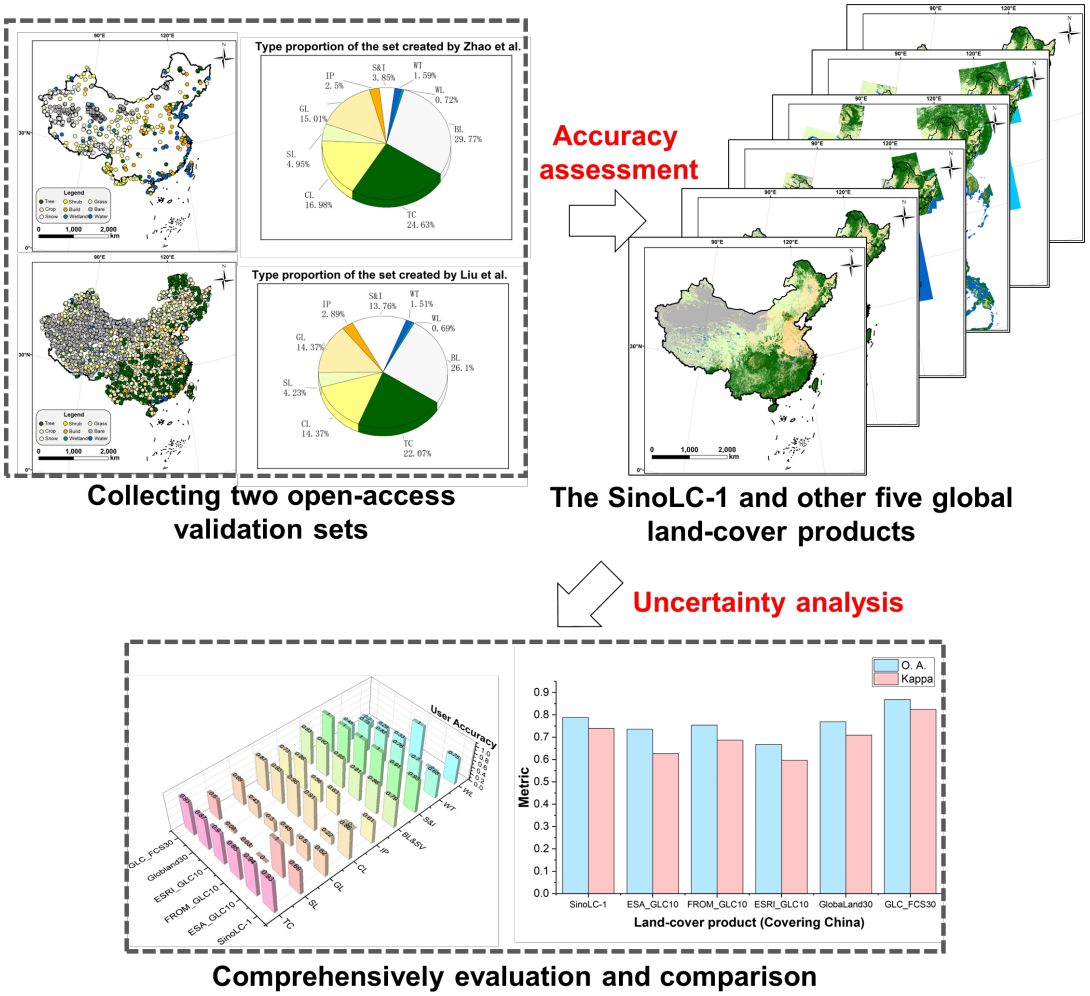

Figure R2-1. The supplemented workflow to evaluate the accuracy and uncertainty of the SinoLC-1 and other five global land-cover products

Secondly, to evaluate the uncertainty of the SinoLC-1 in the Southwest, Northwest, and North regions due to unmatched training data and outdated VHR images, we conducted a more complete accuracy validation based on the two open-access datasets in Section 4.3.2 (Statistical-level validation) Section 4.2.2 (Quantitative comparison with other land-cover products) of the revised manuscript and added a statistical-level error analysis of each land-cover type in Section 4.3.2 (Statistical-level validation). Furthermore, following your concerns in **Comment 11**, we have added a statistical table in Table 8 of the revised manuscript (shown in Table R1 of the response letter) to demonstrate the proportion and coverage of the change areas in each provincial region and added a province-scale change map in Figure 22 of the revised manuscript (shown in Figure R2-22 of the response letter) to illustrate the change rate (2011-2021) of China. Figure R2-2 shows the supplemented workflow to evaluate the error and uncertainty distribution of the SinoLC-1. The detailed material and descriptions are demonstrated in response to **Comments 9 and 11** (pages 19 and 24 of this response letter).

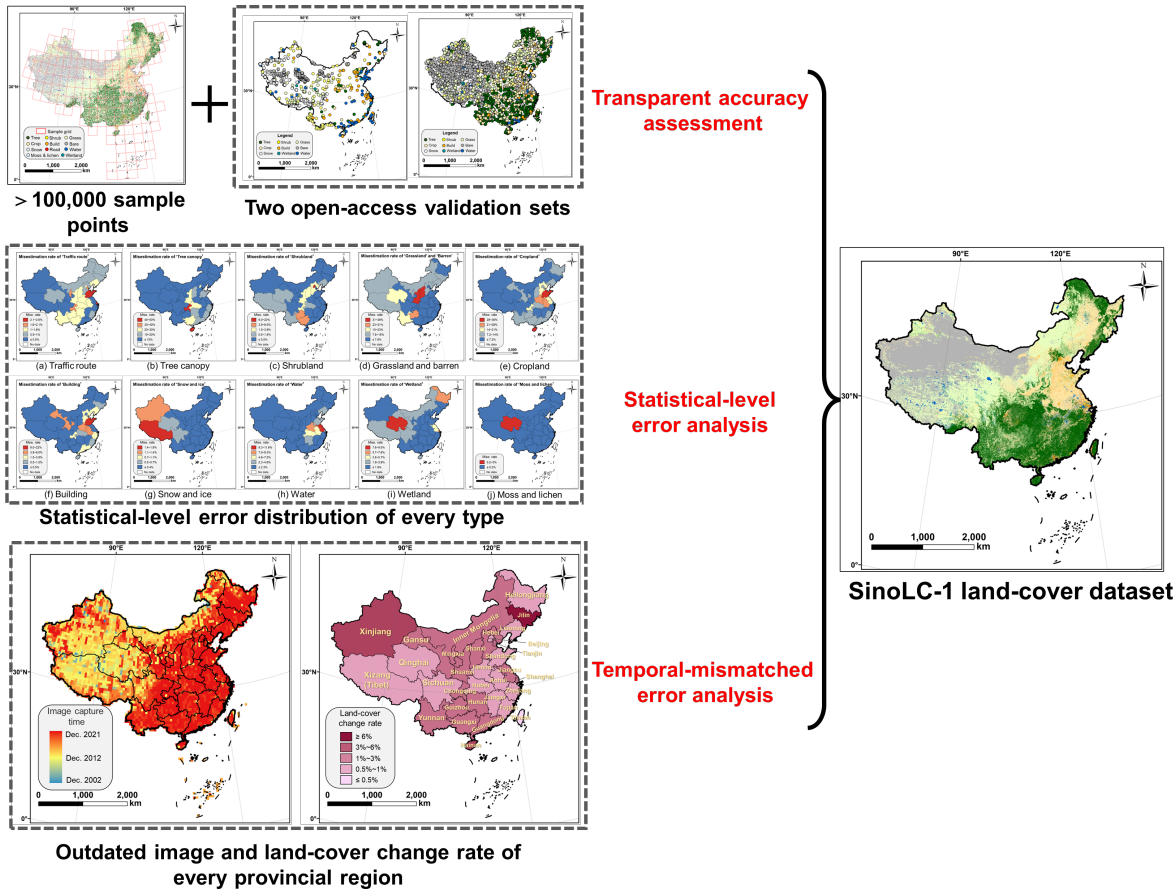

Figure R2-2. The supplemented workflow to evaluate the error and uncertainty distribution of SinoLC-1

(2) Validation uncertainty. The authors manually annotated 106,852 points by visual interpretation results of VHR or HR imagery as validation datasets (Line 296-298). However, the accuracy of visual interpretation might contain considerable uncertainty. For example, ponds/lakes, paddy fields, and wetlands might be mis-interpretated. There are some open-accessed validation datasets (some obtained from field surveys), it would be great if the authors could add more rigorous and transparent validation.

Response:

We are grateful to the reviewer for pointing out this problem. To address it, we first added the VHR samples captured from the 1.07-m Google Earth images for all land-cover types in Figure 6 of the manuscript (Figure R2-3 of the response letter). For each land-cover type, three VHR samples were added to help readers comprehend their characteristics. Secondly, we added two widely used open-access validation datasets (Liu et al., 2019; Zhao et al., 2014) to conduct more rigorous and transparent validation. These validation datasets were created on a basis of multiple data sources and manual verification, reporting a stable quality and high independence. The detailed information of these validation sets is as follows:

(1) Validation set created by Liu et al. DOI: https://doi.org/10.5281/zenodo.3551995.

Liu et al. (2019) created a global land-cover validation set by combining several existing reference datasets, such as the GLCNMO2008 training dataset, VIIRS reference dataset, STEP reference dataset and Global cropland reference data, to guarantee the confidence and objective of the validation samples. Furthermore, high-resolution imagery in Google earth and time-series NDVI, NDSI values of each related point were integrated to obtain the validation datasets.

(2) Validation set created by Zhao et al. DOI: https://doi.org/10.1080/01431161.2014.930202.

Zhao et al. (2014) created a global land-cover validation set with a total of 38,664 sample units by interpreting Landsat images and MODIS EVI time series data, as well as high-resolution images from Google Earth, recording the quality of reference data, and interpreter confidence. Zhao et al. confirmed that the dataset had been carefully improved through several rounds of interpretation and verification by different image interpreters, and checked by one quality controller. Independent test interpretation indicated that the quality control correctness level reached 90% at level 1 land-cove type.

According to the description of the data providers, these validation sets contain two levels of land-cover types, and their spatial distribution and classification system are shown in Figure R2-4, Table R2-1, and Table R2-2.

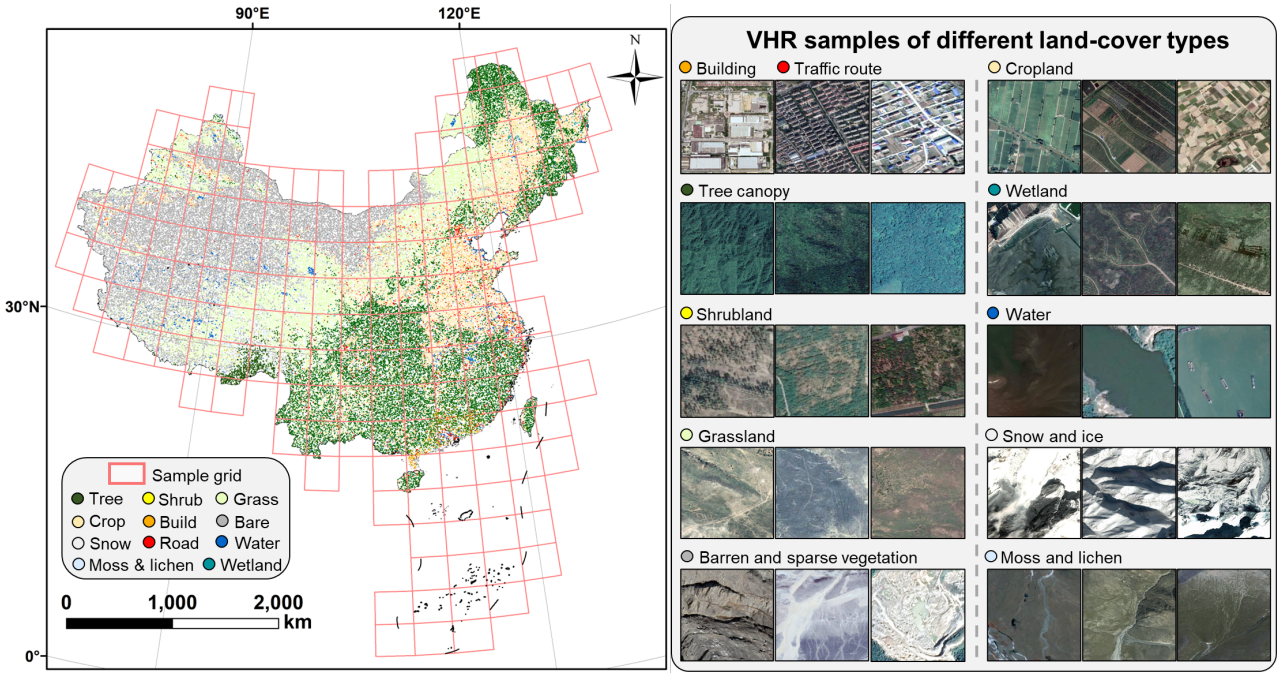

Figure R2-3. Demonstration of the sample grid, VHR samples, and the national validation sample set. Left: the spatial distributions of the sample set (the legend is written in shorter forms). Right: the VHR samples of different land-cover types collected from 1.07-m resolution © Google Earth imagery all around China.

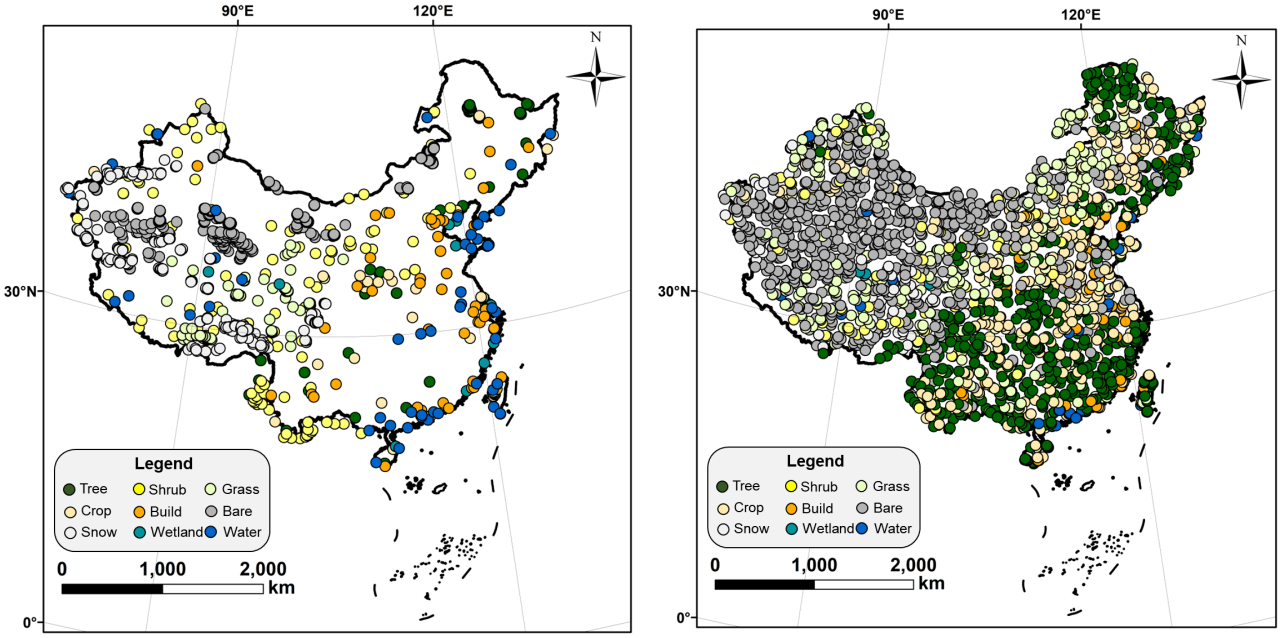

(a) Validation set created by Liu et al.

(b) Validation set created by Zhao et al.

Figure R2-4. Demonstration of two open-access validation set.

Table R2-1. The classification system of the validation set created by Liu et al.

Level 1 type	Level 2 type	Sample count	Total	Proportion (%)
Cropland	Rainfed cropland	44	353	14.33%
	Herbaceous cover	0		
	Irrigated cropland	311		
Forest	Evergreen broadleaved forest	123	542	22.01%
	Deciduous broadleaved forest	303		
	Mixed leaf forest	116		
Shrubland	Shrubland	78	104	4.22%
	Evergreen shrubland	26		
Grassland	Grassland	360	360	14.62%
Wetlands	Wetlands	17	17	0.69%
Impervious surfaces	Impervious surfaces	71	71	2.88%
Bare areas	Sparse vegetation	285	641	26.03%
	Bare areas	329		
	Consolidated bare areas	3		
	Unconsolidated bare areas	24		
Water body	Water body	37	37	1.50%
Permanent ice and snow	Permanent ice and snow	338	338	13.72%

Table R2-2. The classification system of the validation set created by Zhao et al.

Level 1 type	Level 2 type	Sample count	Total	Proportion (%)
Crop	Rice	3	353	16.98%
	Greenhouse	1		
	Other	349		
Forest	Broadleaf	303	512	24.63%
	Needleleaf	81		
	Mixed	114		
	Orchard	14		
Grass	Managed	0	312	15.01%
	Nature	312		
Shrub	Shrub	103	103	4.95%
Wetland	Grass	15	15	0.72%
	Silt	0		
Water	Lake	7	33	1.59%
	Pond	19		
	River	7		
	Sea	0		
Impervious	High albedo	19	52	2.50%
	Low albedo	33		
Bare land	Saline-Alkali	10	619	29.77%
	Sand	138		
	Gravel	303		
	Bare-cropland	89		
	Dry river/lake bed	2		
	other	77		
Snow and Ice	Snow	80	80	3.85%
	Ice	0		

Based on two open-access validation sets, we calculated the confusion matrix of SinoLC-1 and further validated its producer accuracy (P.A.), user accuracy (U.A.), overall accuracy (O.A.), and kappa coefficient. As shown in Table R2-3 and Table R2-6, the O.A. of the SinoLC-1 validated on the validation sets created by Liu et al. and Zhao et al. are 78.80% and 64.69%, respectively. The Kappa of the SinoLC-1 validated on the validation sets created by Liu et al. and Zhao et al. are 0.7394 and 0.5588, respectively.

Furthermore, to illustrate more detailed assessment results, Figure R2-5 shows the corresponding confusion proportions for each considered land-cover type of the SinoLC-1 validated on two sets. In addition, to assess the SinoLC-1 more rigorously and transparently, we used these validation sets to validate the accuracy of five comparative land-cover datasets, and the quantitative results are shown in Table R5. With the validation set created by Liu et al, all products have a higher O.A. and the SinoLC-1 ranks second with an O.A. of 78.81%. With the validation set created by Zhao et al, all products have an O.A. of around 60%, and the SinoLC-1 ranks second with an O.A. of 64.69%.

According to your consideration in **Comment 9** (recommending us to add numerical statistics results to compare the performance of different land-cover products in China), we made a more detailed comparison and analysis in response to **Comment 9** to compare the SinoLC-1 and the other five products more comprehensively.

Table R2-3. Confusion matrix for the SinoLC-1 according to the validation set created by Liu et al.

Classification	TC	SL	GL	CL	IP	BL&SV	S&I	WT	WL	Total	P.A. (%)
Tree Cover	421	5	80	32	0	2	1	1	0	542	77.68
Shrubland	7	34	32	2	0	27	2	0	0	104	32.69
Grassland	2	2	342	0	0	7	0	0	0	353	96.88
Cropland	5	1	3	316	29	3	0	3	0	360	87.78
Impervious	7	0	3	7	51	3	0	0	0	71	71.83
Barren &Sparse veg.	1	7	12	0	0	616	5	0	0	641	96.10
Snow and ice	1	0	78	0	0	121	136	2	0	338	40.24
Water	7	0	0	5	3	1	0	19	2	37	51.35
Wetland	0	0	1	4	0	1	2	3	6	17	35.29
Total	451	49	551	366	83	781	146	28	8	2463	
U.A. (%)	93.35	69.39	62.07	86.34	61.45	78.87	93.15	67.86	75.00		
O.A. (%)						78.80					
Kappa						0.7394					

Note: TC=Tree cover; SL=Shrubland; GL=Grassland; CL=Cropland; IP=Impervious (Building and traffic route); BL&SV=Barren and sparse vegetation; S&I=Snow and ice; WT=Water; WL=Wetland

Table R2-4. Confusion matrix for the SinoLC-1 according to the validation set created by Zhao et al.

Classification	TC	SL	GL	CL	IP	BL&SV	S&I	WT	WL	Total	P.A. (%)
Tree Cover	376	13	60	35	6	7	1	5	9	512	73.44
Shrubland	10	34	33	3	0	21	2	0	0	103	33.01
Grassland	37	2	215	20	3	33	0	1	1	312	68.91
Cropland	83	1	36	191	18	21	0	2	1	353	54.11
Impervious	3	0	4	13	29	3	0	0	0	52	55.77
Barren &Sparse veg.	13	7	109	62	6	411	5	5	1	619	66.40
Snow and ice	1	0	5	0	0	8	65	1	0	80	81.25
Water	6	0	0	7	2	2	0	16	0	33	48.48
Wetland	0	0	2	0	1	2	2	0	8	15	53.33
Total	529	57	464	331	65	508	75	30	20	2079	
U.A. (%)	71.08	59.65	46.34	57.70	44.62	80.91	86.67	53.33	40.00		
O.A. (%)						64.69					
Kappa						0.5588					

Note: TC=Tree cover; SL=Shrubland; GL=Grassland; CL=Cropland; IP=Impervious (Building and traffic route); BL&SV=Barren and sparse vegetation; S&I=Snow and ice; WT=Water; WL=Wetland

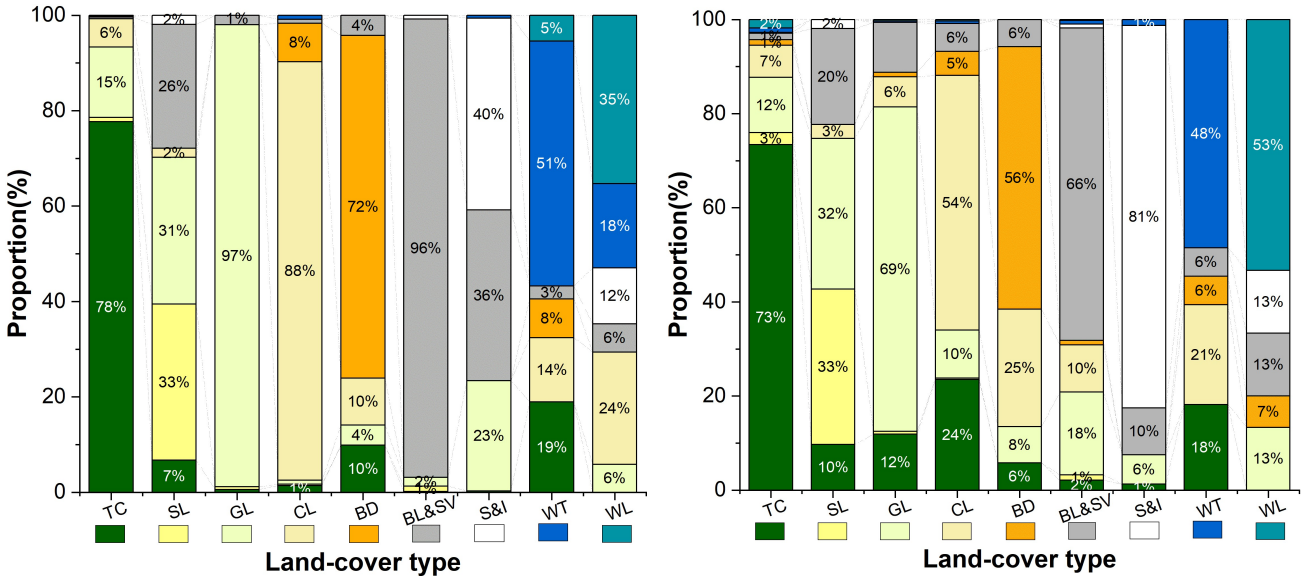

(a) Confusion proportions for land-cover type of the SinoLC-1 validated with the set created by Liu et al.

(b) Confusion proportions for land-cover type of the SinoLC-1 validated with the set created by Zhao et al.

Figure R2-5. Confusion proportions of the validation results.

Table R2-5. Quantitative comparison between the SionLC-1 and other five land-cover products.

Metric / Dataset	Validation set of Zhao et al.		Validation set of Liu et al.	
	O. A.	Kappa	O. A.	Kappa
SinoLC-1	0.6469	0.5588	0.7881	0.7394
ESA_GLC10	0.6646	0.5722	0.7356	0.6269
FROM_GLC10	0.6411	0.5942	0.7538	0.6871
ESRI_GLC10	0.6232	0.5210	0.6675	0.5972
GlobaLand30	0.6209	0.5285	0.7694	0.7090
GLC_FCS30	0.5778	0.4675	0.8684	0.8241

The cited references of this response are as follows:

Zhao, Y., Gong, P., Yu, L., Hu, L., Li, X., Li, C., Zhang, H., Zheng, Y., Wang, J., Zhao, Y. and Cheng, Q. (2014). Towards a common validation sample set for global land-cover mapping. International Journal of Remote Sensing, 35(13), 4795-4814. https://doi.org/10.1080/01431161.2014.930202

Liu, L., Gao, Y., Zhang, X., Chen, X., & Xie, S. (2019). A Dataset of Global Land Cover Validation Samples (Version v1) [Data set]. Zenodo. https://doi.org/10.5281/zenodo.3551995

(3) Line 25: "SinoLC-1 conformed closely to the official survey reports", this expression is vague, needs statistical values to support how close.

Response:

Thank you for the suggestion. To be clearer and in accordance with your concerns, we have added a histogram of the national misestimation rate, as shown in Figure 23 (c) of the revised manuscript (Figure R2-6 (a) of the response letter), to visualize the statistical assessment of every land-cover type containing in SinoLC-1. Furthermore, we calculated the Frequency Weighted Misestimation Rate (FWMR) of SinoLC-1 to measure the overall proximity of SinoLC-1 to the official survey reports. Referring to the calculation of Frequency Weighted Intersection over Union (FWIoU) (Long et al., 2015), FWMR is calculated by multiplying the misestimation rate of each land-cover type by their proportions shown in Figure R2-6 (b) and summing them up. Formally, the FWMR can be written as:

$$FWMR = \sum_{c=1}^{11} p_c m_c,$$

where c represents the land-cover types counting from 1 to 11 (from 'traffic route' to 'Moss and

lichen'), p_c represents the class proportion of c land-cover type, and m_c represents the misestimation rate of c land-cover type.

According to the results shown in Figure R2-6 (a), the national misestimation rates of all land-cover types are under 11%, and the overall FWMR is 6.4%. Based on the analysis, we have revised the expression describing the overall proximity of SinoLC-1 to the official survey reports in the Abstract, Section 4.3.2 (Statistical-level validation), and Section 6 (Conclusion) of the manuscript.

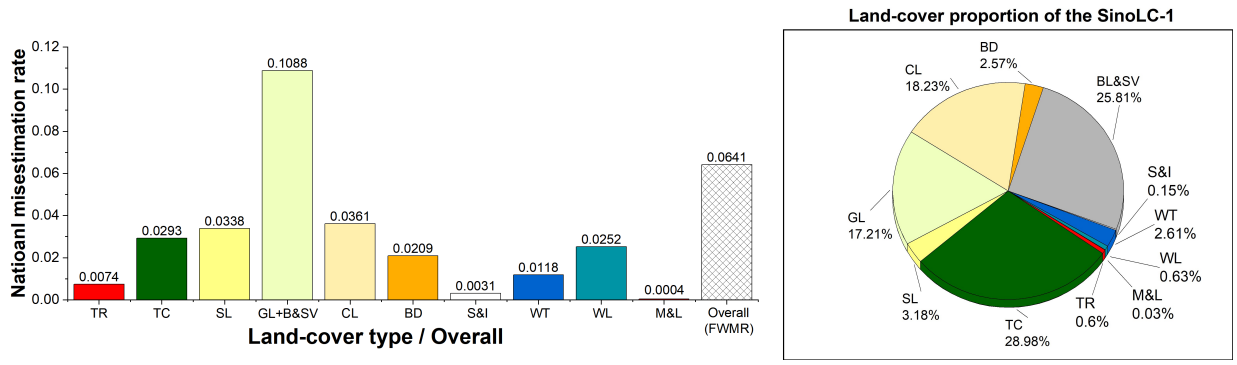

(a) National misestimation rate of every land-cover type across China (b) Class proportion of the SinoLC-1 dataset.

Figure R2-6. National misestimation rate and class proportion of the SinoLC-1 dataset.

The cited reference of this response is as follow:

Long, J., Shelhamer, E., & Darrell, T. (2015). Fully convolutional networks for semantic segmentation. In Proceedings of the IEEE conference on computer vision and pattern recognition, 3431-3440.

(4) Line 275-276: "the predicted batches were seamlessly merged into the land-cover tiles by taking the average predicted values of the overlapped areas", since the land cover is categorical data, it would be more reasonable to take the majority instead of the average.

Response:

Thanks for your constructive feedback. For common majority-voting process, three or more prediction results are required. For the overlapping part of two prediction results, we calculated the average of probability matrix for the overlapping areas, and then for every pixel located in the overlapping areas, we take the class with maximum predicted probabilities among all land-cover classes as the final prediction results. According to your comment, we would like to explain the seamless mapping and merging process more clearly. In this response letter, we supplemented

Figure R2-7 to illustrate the processing process of overlapped areas and Figure R2-8 to show a simple example to explain how the final results are obtained via two overlapped batches.

For each image tile (6000×6000 pixels) shown in Figure R2-7, adjacent image batches (256 ×256 pixels) with 128 pixels overlapped areas are taken as the input of a well-trained model to obtain two prediction matrices $\mathbf{M}_1$ and $\mathbf{M}_2$, where each matrix has a prediction probability with the sizes of 11×256×256 (Class×Height×Width). Subsequently, the average value of the overlapped parts on each class (e.g., tree, building, water, etc.) is calculated to obtain the average matrix $\mathbf{M}_{avg}$. Finally, as shown in Figure R2-8, the maximum value of each pixel in $\mathbf{M}_{avg}$ is taken among each class channel to obtain the final land-cover mapping results. Based on this process, the problem of edge mismatch between adjacent prediction results is alleviated to a certain extent, assisting us to obtain seamless and continuous land-cover maps.

In order to provide a clearer explanation of this process in the revised manuscript, we have supplemented the expression in Section 3.2.2 (Seamless mapping and merging) and modified Figure 5 of the manuscripts (shown in Figure R2-9 of the response letter).

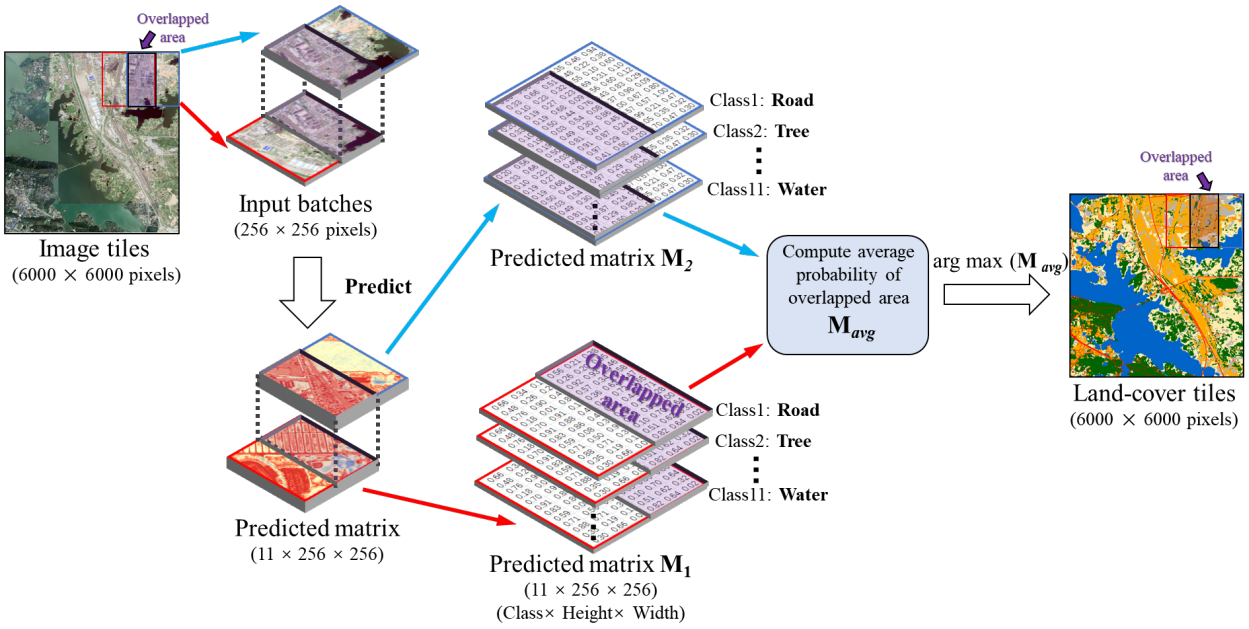

Figure R2-7. Demonstration of the processing process of overlapped areas

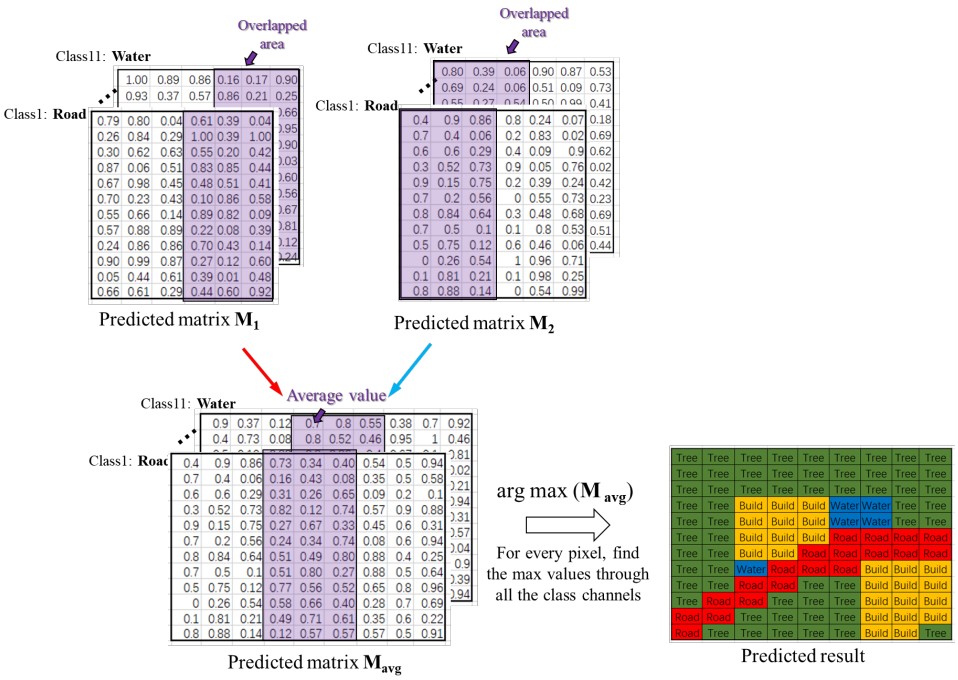

Figure R2-8. Demonstration of a simple example to explain how the final results are obtain via two overlapped batches.

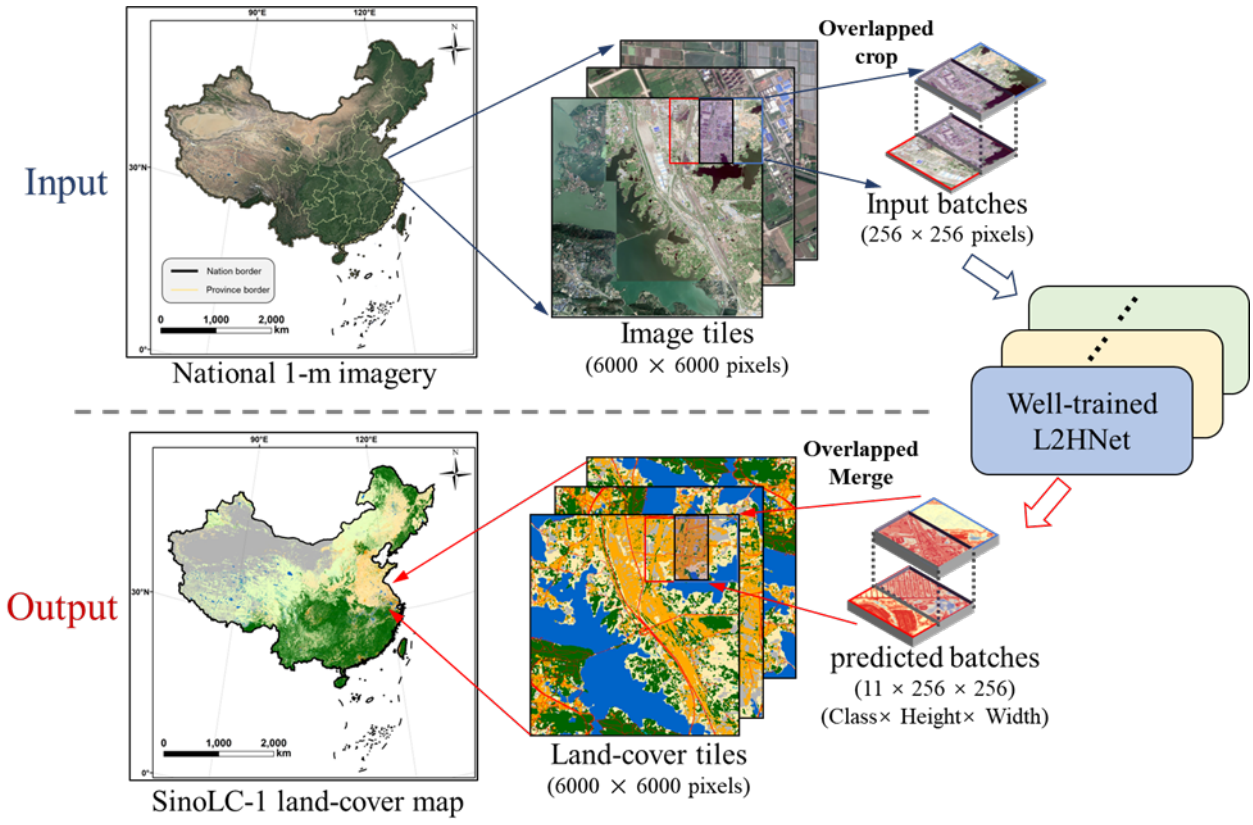

Figure R2-9. Demonstration of the mapping and merging for producing SinoLC-1. The VHR remote sensing images in the figure are from © Google Earth 2021

(5) Figure 7: the bar showed the sample number instead of the proportion. It would be better to show the proportion of the validation samples of each type account for all sample points (106, 852) and the area proportion of each land-cover type of China in the SinoLC-1 dataset.

Response:

Thank you for the constructive comments which can improve the quality and reasonability of the manuscript. According to your comments, we modified the histogram shown in Figure 7 of the previous manuscript (Figure R2-10 (a) of the response letter) into the pie chart which can better demonstrate the proportion of each land-cover type. Furthermore, as shown in Figure R2-10 (b), we supplemented the pie chart of the land-cover proportion in the SinoLC-1 dataset. Based on the modified Figure 7 of the revised manuscript, the land-cover proportion of selected sample points in the validation set is relatively similar to the SinoLC-1 dataset, further indicating that the ~100,000 sample points have reasonable class distribution.

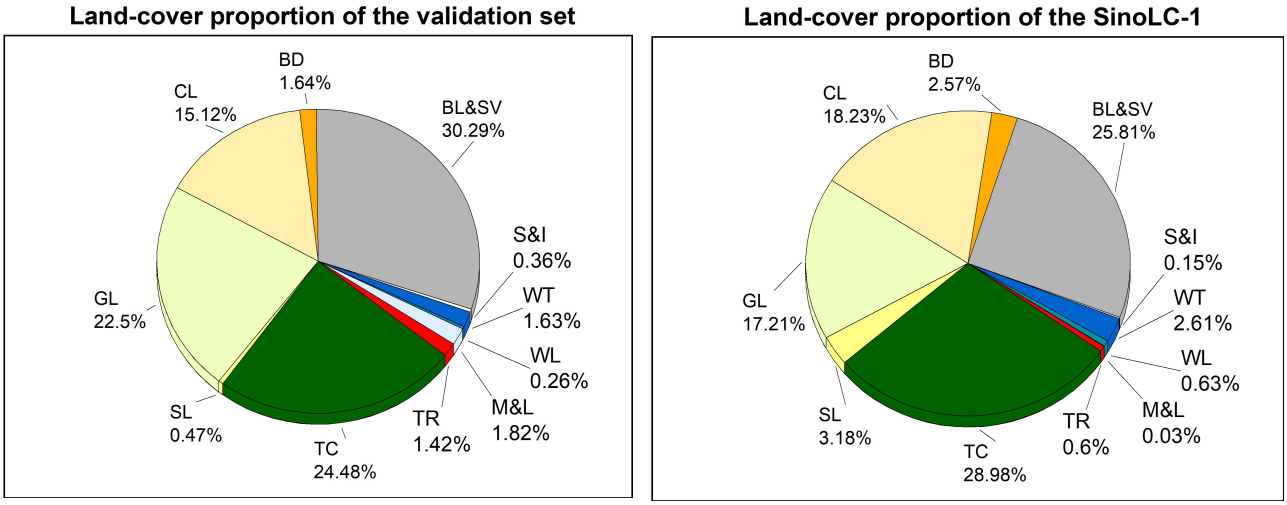

(a) Class proportion of the national validation sample set. (b) Class proportion of the SinoLC-1 land-cover dataset.

Figure R2-10. Land-cover proportion of the national validation sample set and the produced SinoLC-1 land-cover dataset.

(6) Figure 8: the legend is missing.

Response:

Thank you for your constructive feedback. We have supplemented the legends to Figures 8 of the revised manuscript (Figure R2-11 of the response letter). Furthermore, to improve the visualization of the qualitative comparison between the SionLC-1 and other land-cover datasets, we also supplemented the legends to all maps shown in Figures 13 and 14 of the manuscript (Figure R2-12 and Figure R2-13 of this respond letter).

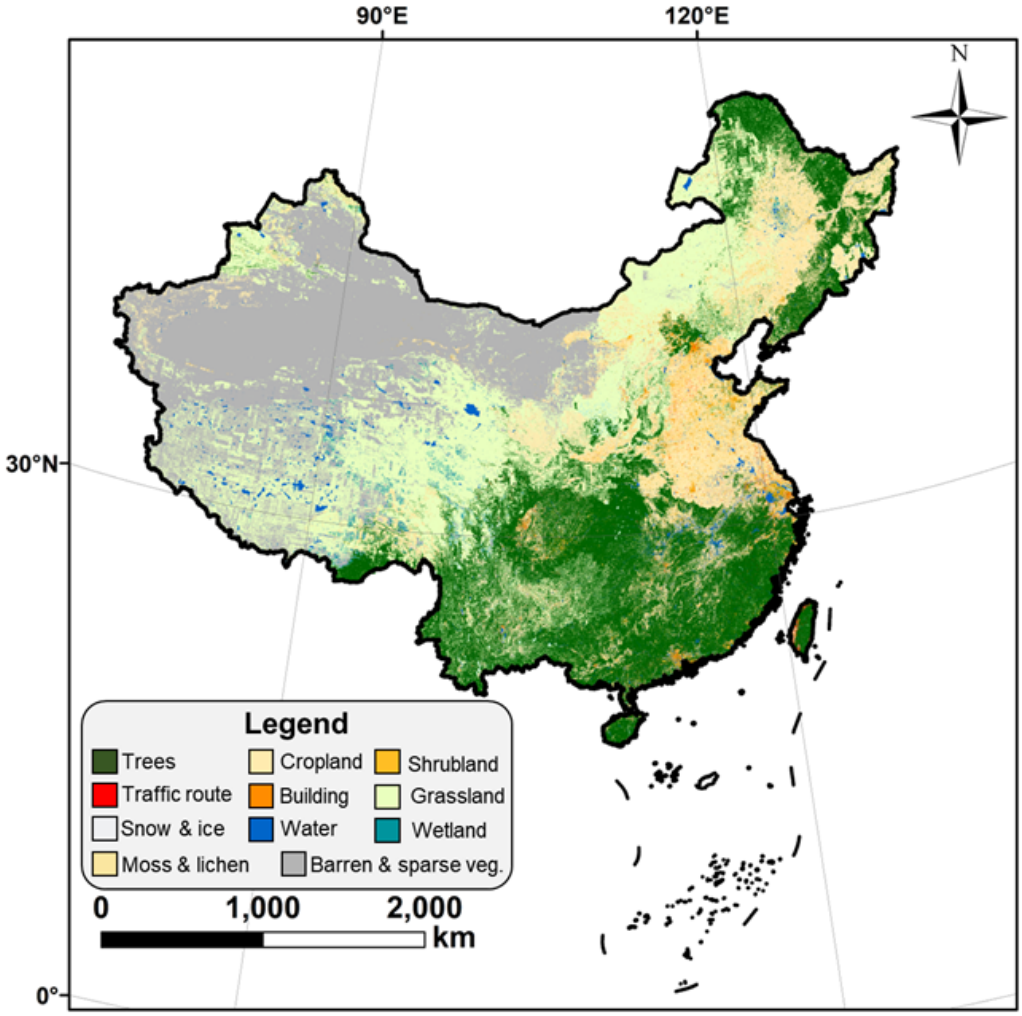

Figure R2-11. Demonstration of the SinoLC-1: a 1-meter-resolution national-scale land-cover map of China.

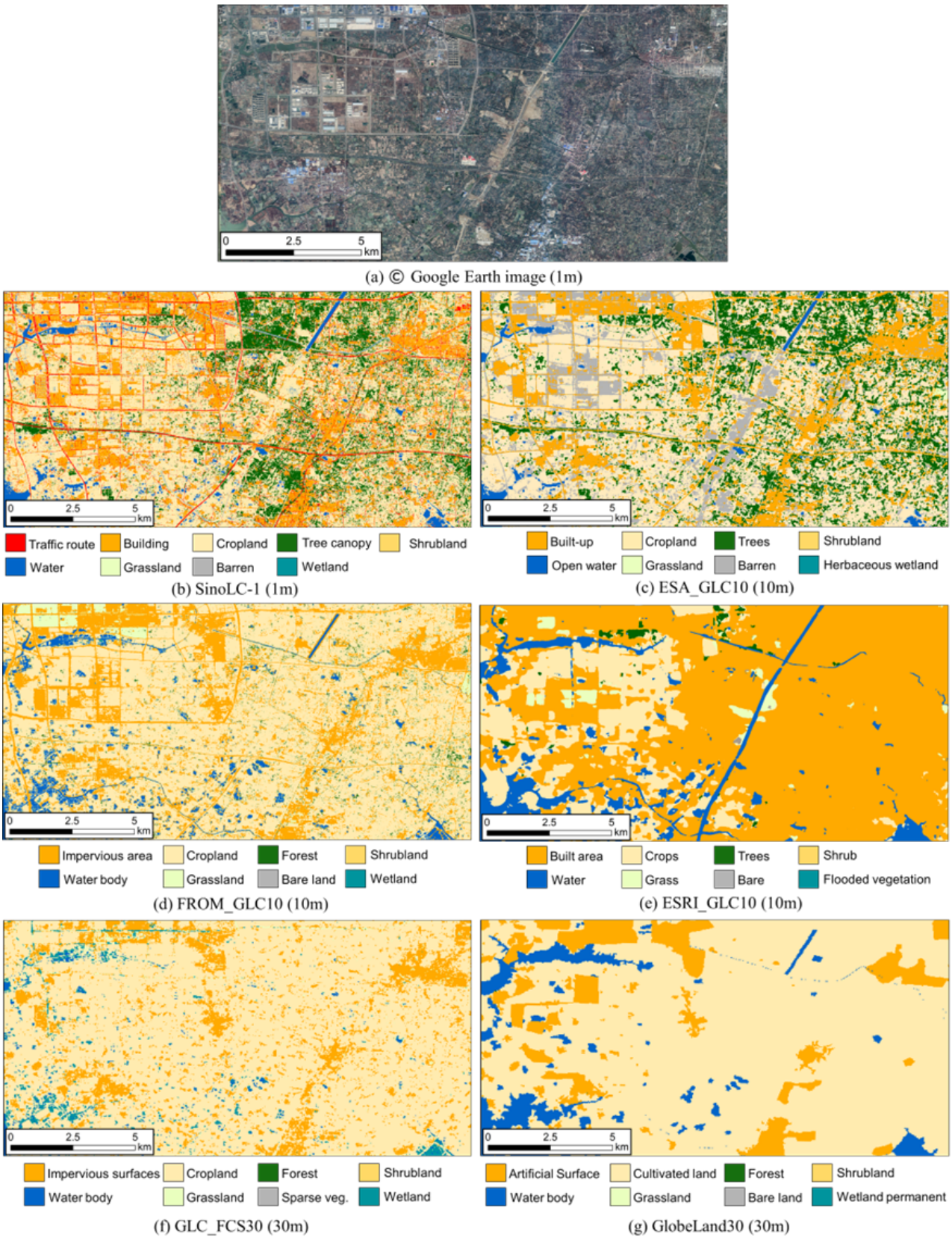

Figure R2-12. Demonstration of the visual comparison for Changzhou City, Jiangsu Province. The VHR remote sensing image in the figure is from © Google Earth 2021.

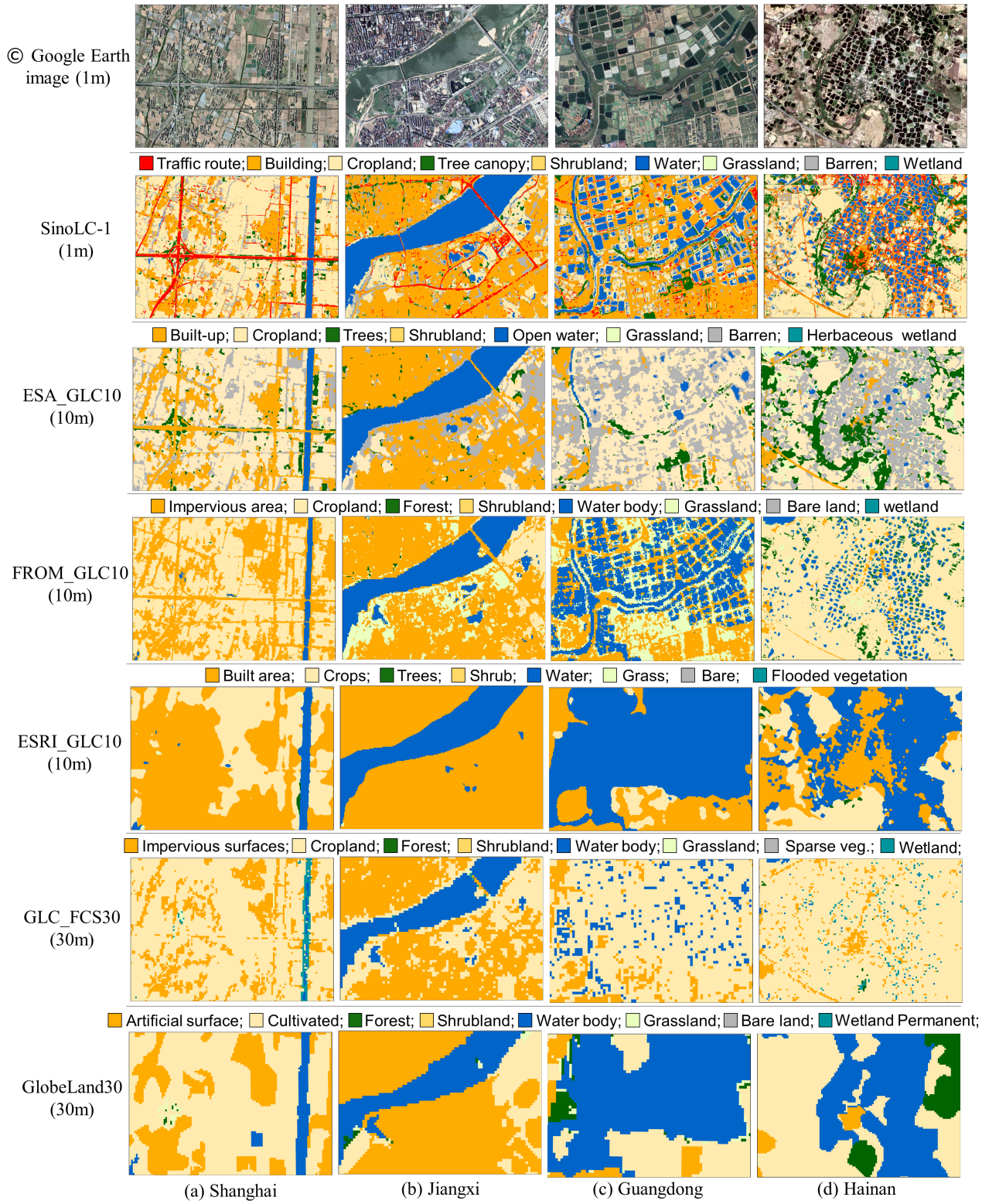

Figure R2-13. Demonstrations of the visual comparison for four typical regions. The VHR remote sensing images in the figure are from © Google Earth 2021.

(7) Line 409-412: The expression is not clear, please clarify which types showed higher accuracies (O.A. and kappa), and which types showed low accuracies.

Response:

Thank you for the comment. We have clarified the exact land-cover types that showed higher and lower accuracies in Section 4.3.1 (Pixel-level sample validation). To describe the analysis results in a more understandable way, the descriptions of the revised manuscript have been revised to ‘

By combining the class proportion of the validation sample set shown in Figure 7and the confusion matrix shown in Table 6 and Figure 19, the quantitative results of the basic land-cover types (i.e., the types of tree canopy, grassland, cropland, barren & sparse vegetation, and water), which have easily distinguishable features and occupy a large area in China, report higher accuracies and have a small proportion of misclassification. By contrast, the land-cover types (i.e., the types of traffic route, moss & lichen, and snow & ice), which occupy a small area, obtain relatively low accuracies and have a large proportion of misclassification.’

(8) Figure 15: Adding the numerical values of confusion proportions to this figure would provide more quantitative information.

Response:

Thank you for the constructive feedback for improving the quantitative information of the figure. We have added the numerical values in Figure 15 of the previous manuscript (Figure R2-14 of this response letter).

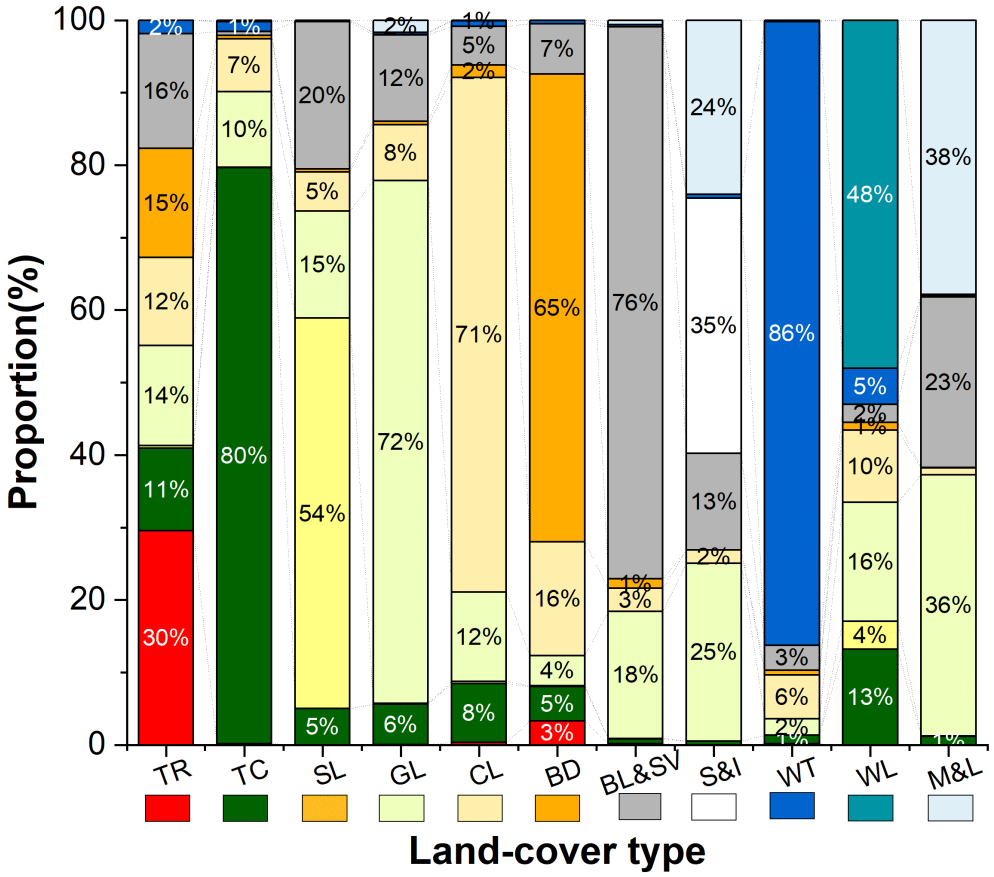

Figure R2-14. Confusion proportions for each land-cover type in the SinoLC-1 validation scheme.

(9) 3.2 section belongs to Results, but almost no numerical statistics were shown to support the descriptions.

Response:

We are grateful to the reviewer for pointing out this problem. In the previous manuscript, Section 4.2 (Qualitative comparison with other land-cover products) focused on the qualitative and visual comparison based on one large-scale demonstration area (shown in Figure 13 of the manuscript) and four region-scale areas (shown in Figure 14 of the manuscript). To conduct a more rigorous comparison and quantitative analysis, we added two widely used open-accessed validation datasets (Liu et al., 2019; Zhao et al., 2014) to conduct validation and comparison of the SinoLC-1 and other five products across China. Moreover, we added a subsection of 'Quantitative comparison with other land-cover products' in Section 4.2.2 to make the comparison more scientific and transparent. Detailed information of these two open-access validation sets has been introduced in **Comment 2**. For clearer expression, we mark the validation set created by Liu et al. (2019) as S1 and mark the set created by Zhao et al. (2017) as S2. Figure R2-15 and Figure R2-16 show the spatial distribution of two validation sets among five comparative products in China.

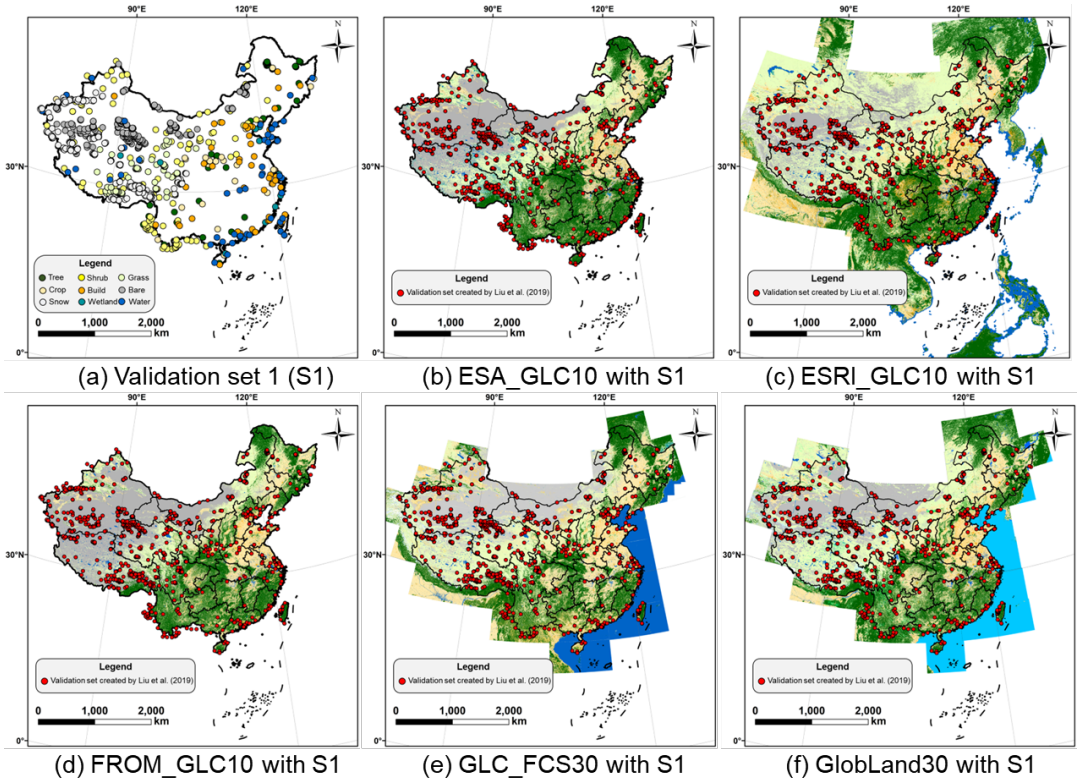

Figure R2-15. Demonstration of five comparison products and the validation set (S1) created by Liu et al.

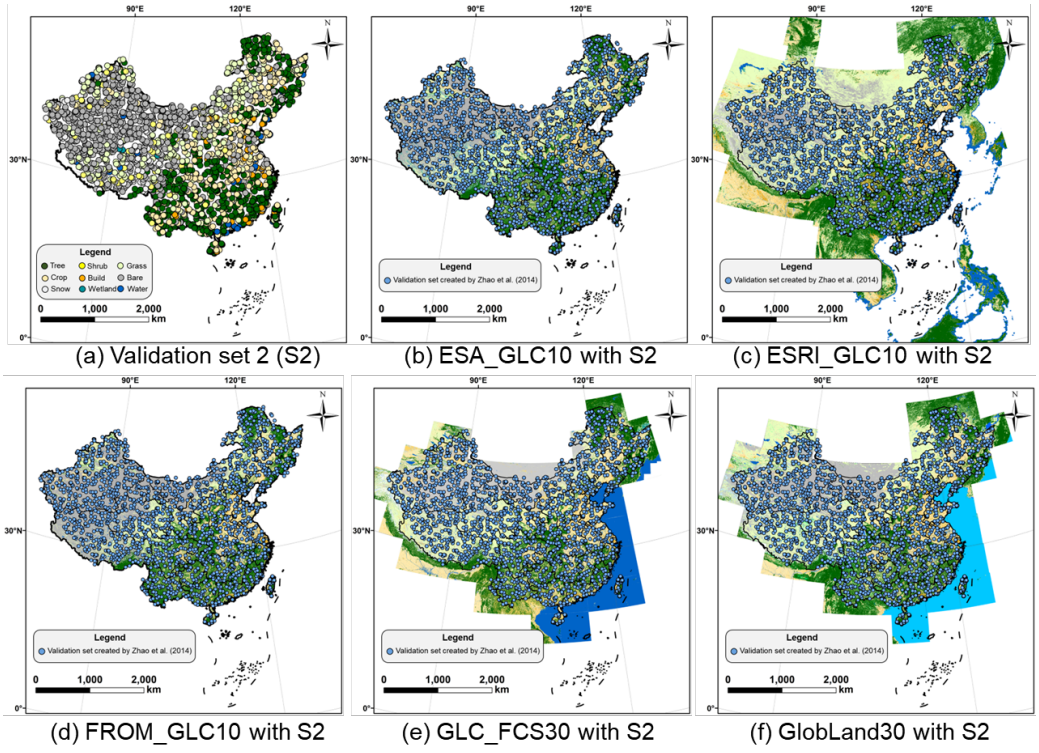

Figure R2-16. Demonstration of five comparison products and the validation set (S2) created by Zhao et al.

Based on the two validation sets, we compared the O.A. and Kappa between the SinoLC-1 and the other five products. The comparison results are shown in Table R2-5 and Figure R2-17. From the quantitative comparison, the SinoLC-1 has the second highest O.A. on two validation sets where the SinoLC-1 has a O.A. of 0.6469 with S1 (lower than the 10-meter ESA_GLC10) and has an O.A. of 0.7881 with S2 (lower than the 30-meter GLC_FCS30). Furthermore, we compared the U.A. of every considered type between the SionLC-1 and the other five products in Figure R2-18. From the results shown in Figure R2-18 (a), the SinoLC-1 has the second highest U.A. in types of 'Tree canopy', 'Shrubland', 'Grassland', and 'Wetland' compared to the other five products, and has the U.A. of 'Cropland' and 'Impervious surface' surpassing the average of other five products. From the results shown in Figure R2-18 (b), the SinoLC-1 has the highest U.A. in types of 'Shrubland' and 'Grassland', and has the U.A. of 'Snow and ice' and 'Wetland' surpassing the average of the other five products.

In general, by quantitatively comparing the SinoLC-1 product with five widely used land-cover products on two open-access validation datasets, the produced SinoLC-1 shows acceptable confusion proportion among land-cover types and has competitive accuracy among the other land-cover products across China.

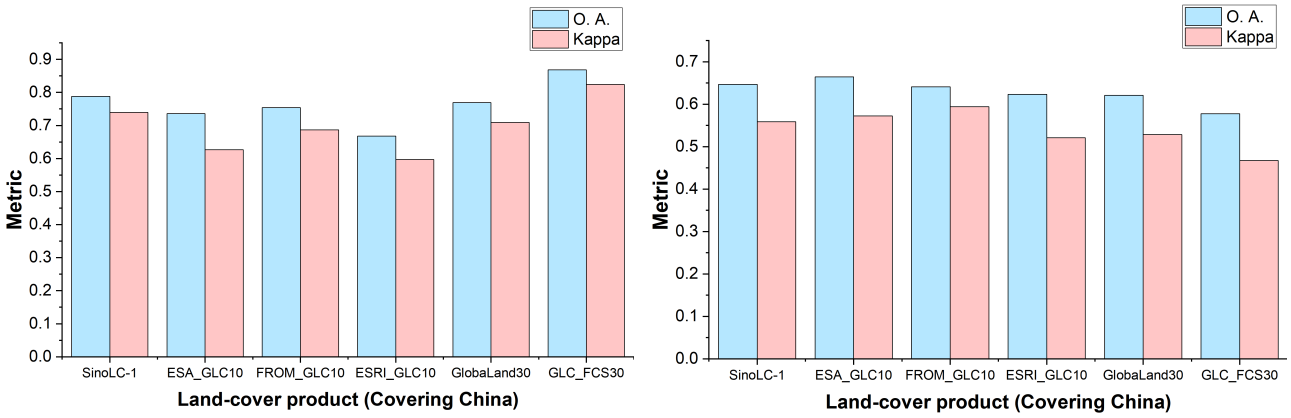

(a) The validation results based on S1 (b) The validation results based on S2

Figure R2-17. The quantitative validation and comparison of the SinoLC-1 and other five products

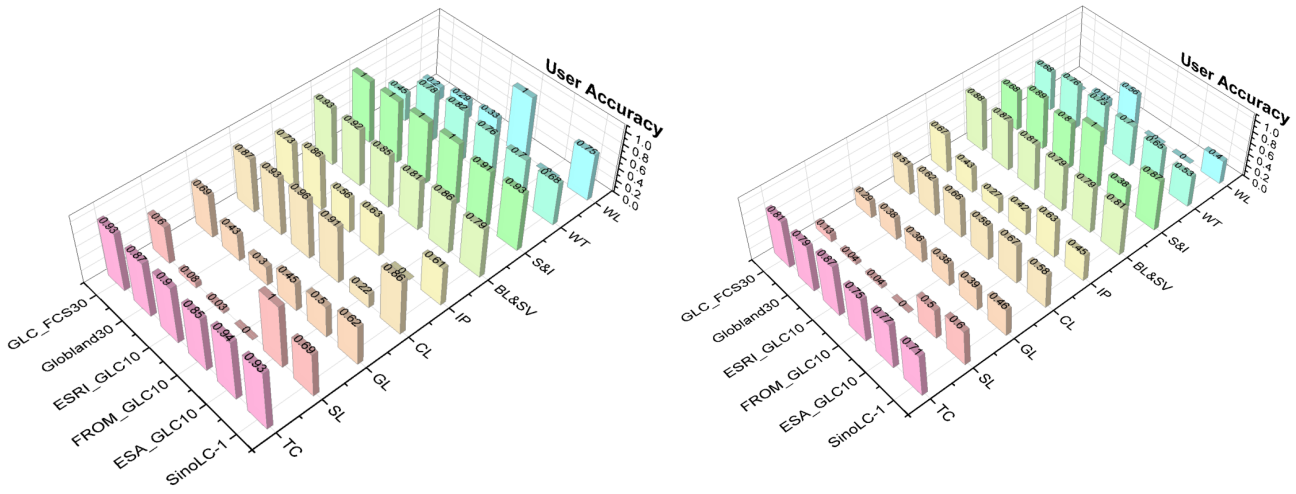

(a) The U.A. comparison based on S1 (b) The U.A. compassion based on S2

Figure R2-18. The U.A. comparison of the SinoLC-1 and other five products.

(10) Figure 18, the left figure (a) showed the misestimated area, while it would be more comparable if it showed the misestimated rate for each land-cover type.

Response:

We are grateful for the suggestion. We agree that the misestimated rate can include more comparable information than the misestimated area between different land-cover types. To be clearer and in accordance with your concerns, we illustrated the misestimated rate of every land-cover type through 31 provincial regions in Figure R2-19 to better visualize the distribution of original results. In the revised manuscript, we have revised Figure 23 (shown in Figure R2-20 of the response letter) by changing the vertical axis of subfigure (a) from 'misestimation area (km^2)' to misestimation rate. Moreover, to visualize the total results of the statistical assessment in China, we have added a histogram of the national misestimation rate shown in Figure 23 (c) of the revised manuscript (Figure R2-20 (c) of the response letter).

In addition, to demonstrate the spatial distribution of the misestimation rate for each land-cover type across China, and to provide more comparable information on the statistical assessment, we have collected the results and added the map of the misestimation rate for every land-cover type in Figure 22 of the revised manuscript (shown in Figure R2-21 of the response letter). From the maps of the misestimation rate, misestimations of some land-cover types show a strong distribution pattern. For example, the misestimation of 'Shrubland' is mainly distributed in the north and southwest of China. The misestimations of 'Grassland' and 'Barren and sparse vegetation' are concentrated in the north, northwest, and southwest of China. The misestimations of 'Cropland' and 'Building' are distributed on the coasts of eastern and southern China. The main misestimation land-cover types distributed in western China (i.e., Qinghai-Tibet Plateau and Xinjiang) are 'Wetland' with a misestimation rate of 7.6% – 9.5%, 'Snow and ice' with a misestimation rate of 0.5% – 1.8%, and 'Moss and lichen' with a misestimation rate of 0.2% – 0.3%.

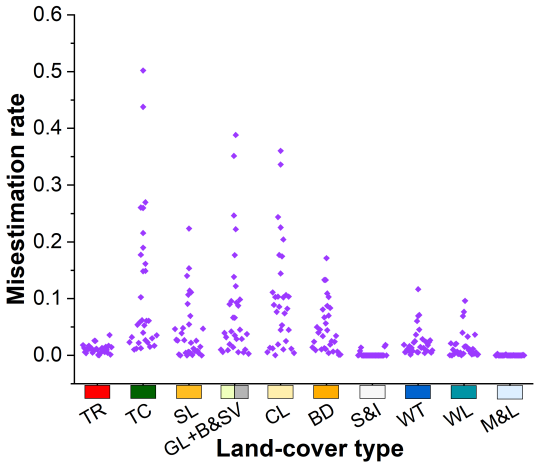

Figure R2-19. Misestimation rate of every land-cover type through 31 provinces in China.

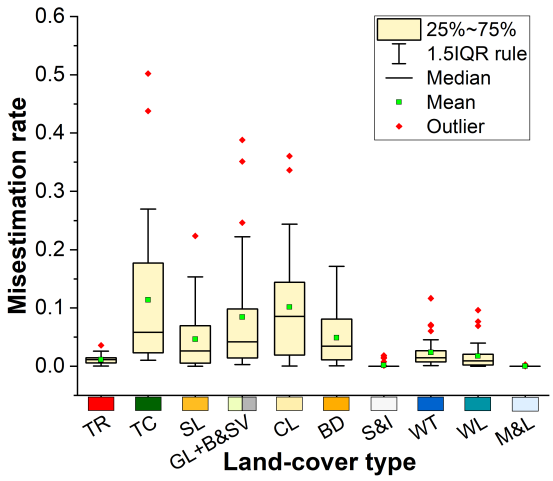

(a) Overall misestimation rate of every land-cover type through 31 provinces in China

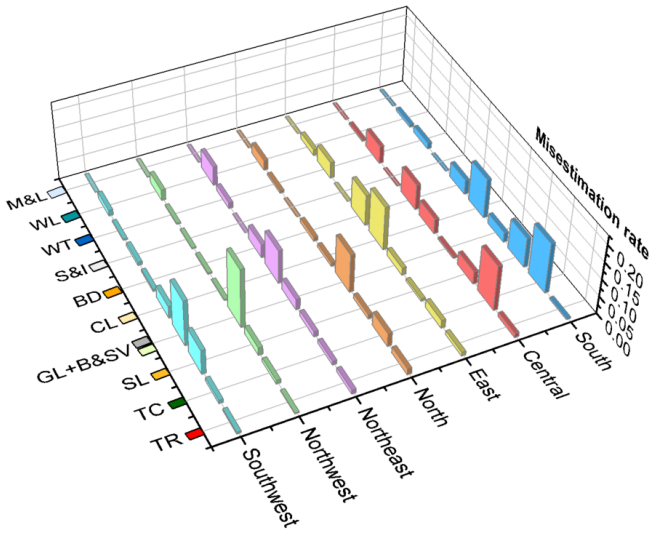

(b) Overall misestimation rate of every land-cover type through seven geographical regions

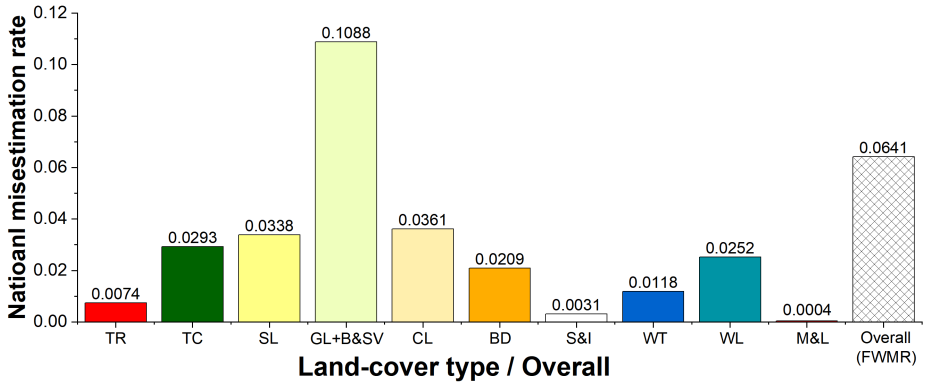

(c) National misestimation rate of every land-cover type across China

Figure R2-20. Overall misestimation distributions in every land-cover type across China.

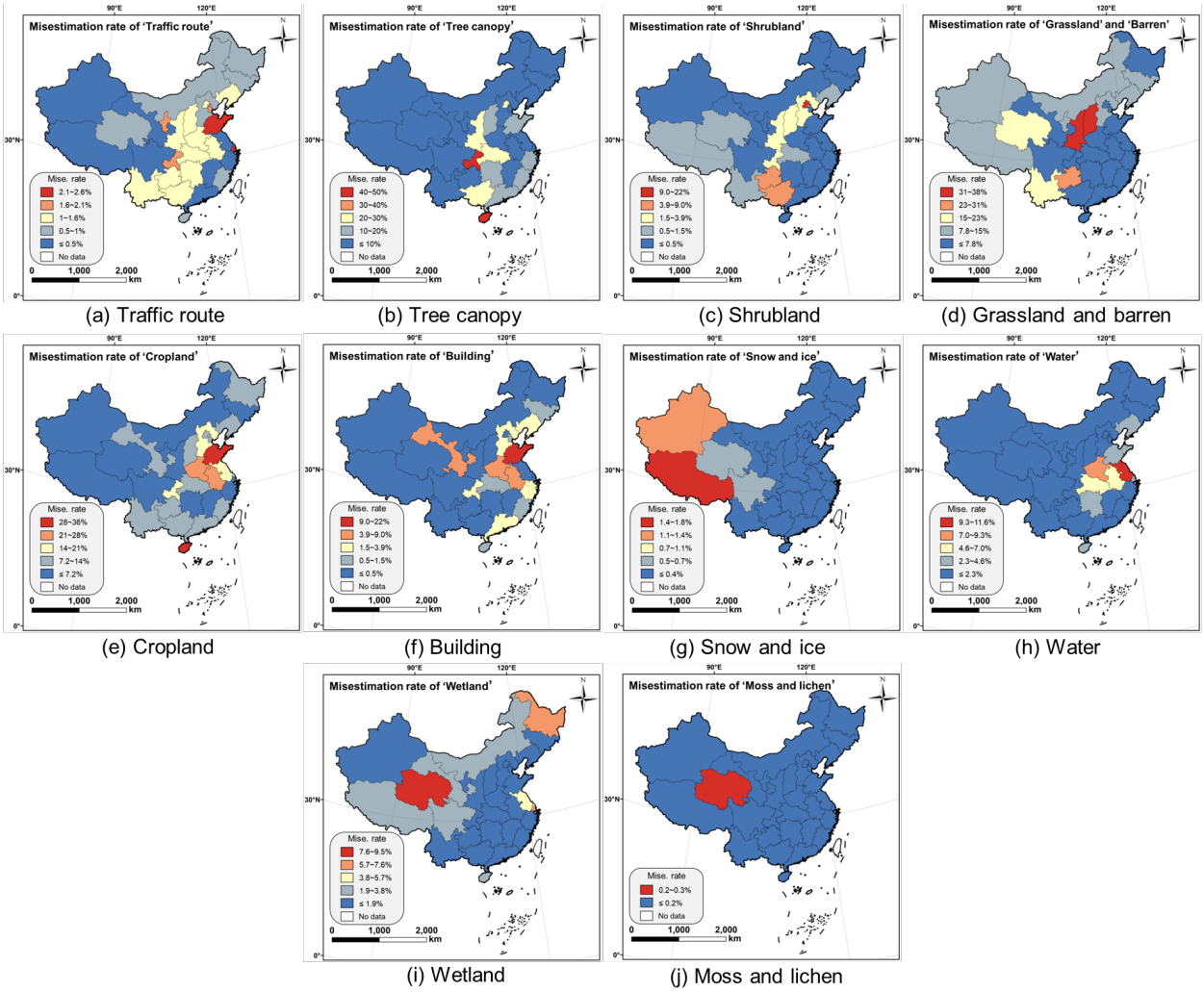

Figure R2-21. The misestimation rate of SinoLC-1 for 31 provinces in China. In every subplot, the statistical comparison between SinoLC-1 and 3rd NLRS data in every land-cover type is illustrated.

(11) Line 480-485: Figure 20 shows significant land-cover changes between 2011 and 2021. It would be better to add a statistical table of the proportion of change areas in each region, which would be helpful to assess the uncertainty in the Southwest, Northwest and North region.

Response:

Thank you for the suggestion that can help visualize the change areas between 2011 to 2021 more clearly and further assist the analysis of uncertainty in the Southwest, Northwest, and North regions. In accordance with your concerns, we have added a statistical table in Table 8 of the revised manuscript (shown in Table R2-6 of the response letter) to demonstrate the proportion and coverage of the change areas in each provincial region.

Table R2-6. The province-scale land-cover change area/rate (2011-2021) of China

Geographical region	Provincial region	Provincial proportion to China's coverage (%)	Change area (km2)	Change rate (%)
South	Hainan	0.37	714.06	2.04
	Guangxi	2.50	3207.55	1.36
	Guangdong	1.89	2107.36	1.18
East	Fujian	1.31	779.53	0.64
	Anhui	1.48	820.93	0.59
	Zhejiang	1.11	719.86	0.69
	Shanghai	0.07	111.32	1.32
	Jiangsu	1.13	1697.93	1.60
	Taiwan	0.38	145.90	0.41
	Jiangxi	1.76	1488.89	0.89
	Shandong	1.64	1416.42	0.92
Central	Hubei	1.96	1852.50	1.00
	Hunan	2.23	2300.15	1.02
	Henan	1.75	1172.96	0.69
North	Shanxi	1.65	2631.97	1.73
	Hebei	1.99	2186.14	1.18
	Beijing	0.17	126.53	0.76
	Inner Mongolia	12.47	13144.22	1.33
	Tianjin	0.13	207.55	1.76
Northeast	Liaoning	1.56	878.47	0.59
	Jilin	0.29	1739.63	0.93
	Heilongjiang	4.98	2849.54	0.61
Northwest	Shaanxi	2.17	2631.97	1.29
	Gansu	4.49	6175.12	1.45
	Xinjiang	17.54	90325.45	5.43
	Ningxia	0.70	1173.43	1.77
	Qinghai	7.61	5695.08	0.79
Southwest	Guizhou	1.86	2702.60	1.67
	Chongqing	0.87	1045.01	1.32
	Xizang (Tibet)	12.68	8792.25	0.81
	Yunnan	4.15	4743.78	1.30
	Sichuan	5.12	3818.27	0.83

Furthermore, we added a province-scale change map in Figure 22 of the revised manuscript (shown in Figure R2-22 of the response letter) to illustrate the change rate (2011-2021) in China. In Figure R2-22 (b), the spatial distribution of the change areas shows that the most significant land-cover changes from 2011 to 2010 are located in the provinces of the south (e.g., Hainan, Guangdong, Guangxi, etc.), north (e.g., Inner Mongolia, Shanxi, Hebei, etc.), northeast (i.e., Jilin), and northwest (e.g., Xinjiang and Gansu). By combining the distribution of outdated images shown in Figure R2-23 and the significant change area shown in Figure R2-22 (b), the outdated VHR images are most probably to cause uncertainty in the mapping results for the northern part of Inner Mongolia and Gansu (i.e., the northern border of China, with the change rate of 1%–3% from 2011 to 2021) and the southern part of Xinjiang (i.e., the Tarim Basin, with the change rate of 1%–3% from 2011 to 2021).

This distribution indicates the areas containing mass outdated images generally had less land-cover change over the years (e.g., Tibet and Qinghai provinces of Southwest China, with a change rate lower than 1%), which limited the uneven effect on the produced results.

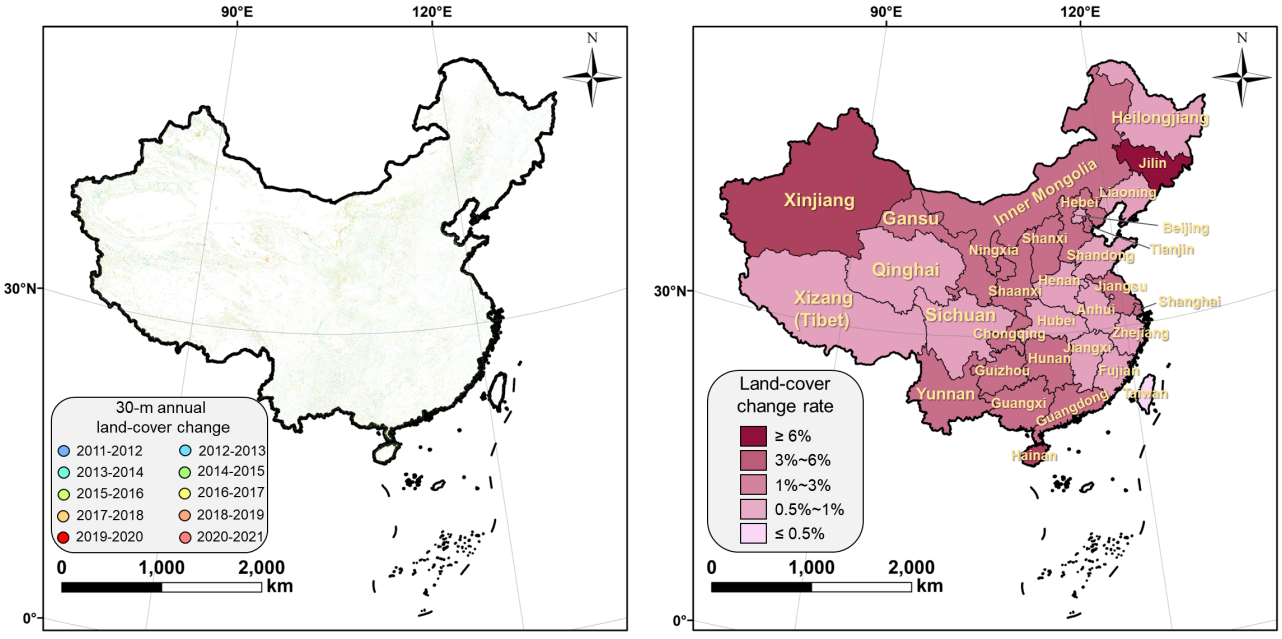

(a) The 30-m annual land-cover change of China from 2011 to 2021

(b) The province-scale land-cover change rate (2011-2021) of China

Figure R2-22. Spatial distribution of 30-m land-cover change in China from 2011 to 2021.

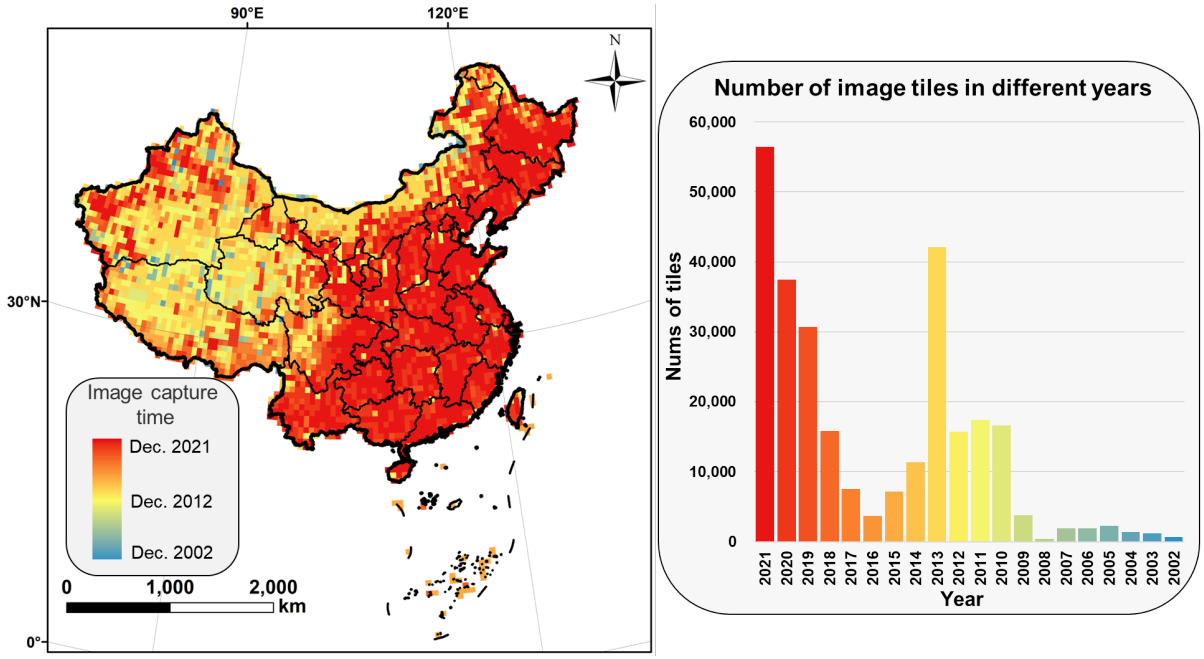

Figure R2-23. Demonstration of the image capture time and the number of image tiles in different years